UCID- 17271-81

E-DIVISION ACTIVITIES REPORT

Compiled by H. H. Barschall

MASTER

July 1981

Lawrence Livermore Laboratory

This is an informal report intended primarily for internal or limited external distribution. The opinions and conclusions stated are those of the author and may or may not be those of the Laboratory.

Work performed under the auspices of the U.S. Department of Energy by the Lawrence Livermore Laboratory under Contract W-7405-Eng-48.

CONTENTS

E-Division Activities Report

July 1981

ABSTRACT

This report describes some of the activities in E (Experimental Physics) Division during the past year. E-Division carries out research and development in areas related to the missions of the Laboratory. Many of the activities are in pure and applied atomic and nuclear physics and in material science. In addition this report describes work on accelerators, microwaves, plasma diagnostics, determination of atmospheric oxygen and of nitrogen in tissue.

INTRODUCTION

E (Experimental Physics) Division carries out basic and applied research in atomic and nuclear physics and in materials science, as well as in other areas related to the missions of the Laboratory. Some of the activities are cooperative efforts with other divisions of the Laboratory, and, in a few cases, with other laboratories. Many of the experiments are directly applicable to problems in weapons and energy, some have only potential applied uses, and others are in pure physics.

E-Division issues an annual report which describes some of the activities in the division during the preceding year. The preceding report (UCID-17271-80) was issued in July 1980. The report gives a brief review of the program of the Division. Not all the activities are included every year. The results of the research are published in detail in the scientific literature and are reported at scientific meetings. References to papers and conference proceedings published since the preceding report of this series are listed in the present report.

LLNL publishes monthly in the Energy and Technology Review (ULRL-52000) descriptions of programs of general interest. Articles describing E-Division activities are reprinted in the E-Division annual reports. The following reprints were included in the previous reports:

Probing Nuclei with LLL's Electron Linear Accelerator (1978)

RTNS: A Tool for Studying Neutron Damage (1978)

The Magnetic-Quadrupole Spectrometer: Studying Neutron Reactions (1978)

Pulsed Sphere Measurements for Weapons and Fusion Reactor Design (1978)

Measuring Hydrogen-Isotope Distribution Profiles (1978)

Nuclear Modeling at the LLL Cyclograaff (1979)

Studying Materials with Positrons (1980)

Probing Nuclear Structure with Improved Electron Scattering Techniques (1980)

Observation of Channeling Radiation (1980)

Measuring the Hydrogen and Helium Produced by Fusion Neutron Reactions (1980)

The present report includes:

Channeling Radiation

ACCELERATORS

Most of the activities of the division are centered around seven accelerators: A 100-MeV electron linear accelerator (Linac), three 400-kV dc high-current accelerators, a 3-MV electrostatic accelerator, a 6-MV tandem electrostatic accelerator, and a 76-cm cyclotron. The cyclotron can be used as an injector for the tandem accelerator (cyclograaff). With these accelerators, beams of neutrons, photons, and charged particles can be produced, and the interaction of these projectiles with nuclei, atoms, and solids is studied.

The oldest of the three 400-kV accelerators ("ICT") produces 25 mA of atomic hydrogen ions, the newer ones ("RTNS II") are designed to produce 150 mA.

Although all the accelerators can serve as neutron sources, most of the neutron experiments use either the Linac or the 400-kV accelerators. The Linac permits the simultaneous study of neutrons of energies from thermal to about 60 MeV by observation of the neutron time-of-flight over distances as long as 250 m. The 400-kV accelerators serve primarily as intense sources of 14-MeV neutrons.

Most of the charged-particle interaction experiments are performed with the cyclograaff. Reactions producing charged particles are studied with the aid of a high resolution broad-range magnetic spectrometer as well as with solid-state detection systems. Low-energy gamma rays produced in charged-particle interactions are detected and their energy is measured in a Ge-Li detector, higher-energy gamma rays in a NaI scintillator with an anticoincidence shield. This latter detector has an unusually large volume:

10 dm^3 for the NaI crystal and 1 m^3 for the plastic scintillator that provides the anticoincidence signal. Neutrons produced in charged-particle reactions are detected and their energy is measured in a well-shielded time-of-flight facility that permits simultaneous observation at 16 angles.

The 3-MV electrostatic accelerator is used for studies of ion-atom collisions and ion interactions with solids.

The tandem electrostatic accelerator, the cyclotron and the oldest 400-kV high current accelerator share the same operating crew so that there are limitations on their simultaneous operation. During the past year the tandem accelerator was operated by itself for about 700 hours and in combination with the cyclotron for 740 hours. Beams produced were protons 68% of the time, deuterons 27%, and alpha particles 5% of the time. The ICT accelerator operated for 1100 hours. The electron linac served as a neutron source for 1900 hours, as a γ-ray source for 400 hours, and for other purposes 200 hours.

Intense Source of 14-MeV Neutrons

The Rotating Target Neutron Source-II (RTNS-II) is a national facility operated for the Fusion Materials Program of the Office of Fusion Energy. Its purpose is to study the effects of fusion neutrons on materials used in the fusion energy program.

During the year covered in this report (July 1980 to June 1981) one of two neutron sources was operated on an 80-hour/week schedule. This includes experiment set-up time. For the same period, a total of 7.4×10^{19} neutrons were produced using 4.7×10^{5} C of beam with an average neutron yield of 1.1×10^{13} neutrons/second. The average neutron source availability was 77%.

Irradiations have been performed for experimenters from twelve laboratories. The largest portion of the irradiation time was devoted to an experiment by the Hanford Engineering Development Laboratory (HEDL). Specimens of ferritic and stainless steel alloys are maintained at ~80° C and ~290° C in a high-vacuum furnace during the irradiation. The largest fluence to be delivered to the samples is 10^{19} neutrons/cm^2. Up to the present a fluence of 6×10^{18} neutrons/cm^2 has been measured at the front surface of the furnace. Included in the irradiation package are both microtensile specimens and Transmission Electron Microscopy (TEM) disks. The latter will be investigated using TEM and microhardness techniques. An irradiation to measure He production in several materials and to determine the spatial distribution of the neutron flux was also completed. In addition short irradiations of mice and of electronic components were performed.

Accelerator Development - Linac

Emittance properties of the electron gun have been studied. Measurements of emittance as a function of output current showed that above 10 A (where most neutron time-of-flight experiments are performed) the emittance is quite good, but it is poor at lower current values (∿2 A) at which most of the long-pulse operation is carried out. Apparently the magnetic-lens/solenoid configuration on the Linac does not give good transmission through the buncher. An alternative lens arrangement has been tried on the test facility. This arrangement will improve the transmission and hence the short-pulse beam current of the Linac. It will be installed soon.

Rf-cavity type beam position monitors have been tested and found to have much better sensitivity than existing position monitors, particularly in the long-pulse mode operation where peak currents are relatively low. A dual-mode rf cavity that will be sensitive to the beam diameter may be useful as a monitor in high-radiation areas where TV cameras cannot be used continuously.

The feasibility of modifying the Linac for use in free-electron laser experiments (λ= 0.5 μm) has been investigated. The requirements included 70-100 MeV beam energy, instantaneous current of at least 100 A in microbunches 3-10 ps in length, microbunch separation of 60 ns or less, with a pulse train lasting at least 10 μs, energy spread of 1% or smaller (FWHM), and normalized transverse emittance of less than 0.04 cm-rad. The cost of the required modifications would be primarily for injector improvements, including subharmonic bunching and a train pulser for the gun, new pulse transformers and extended pulse-forming networks to provide 20 μs rf pulses, improvements in beam diagnostics and beam stability.

A method has been developed to measure the spatial distribution of the neutron beam that is used for cross section measurements. Fissions in a foil of ^{235}U are detected by two position-sensitive multiwire proportional counters to provide beam profiles. The detector is insensitive to gamma and alpha radiation and can be large enough to map the entire beam profile at one time. The counters give nanosecond timing information so that the neutron flux can be measured as a function of neutron energy for the pulsed neutron source.

NUCLEAR PHYSICS

Fission

The nuclides $^{242}Am^{m}$ and ^{245}Cm are two of the major transplutonic elements of concern to such applied problems as actinide burn-up and ^{252}Cf production. Important parameters for determining the reactivity of these fissionable materials are their fission cross sections and the average numbers of neutrons per fission ($\bar{\nu}$).

The fission cross sections of $^{242}Am^{m}$ and ^{245}Cm were measured for neutrons of energies between 1 and 10 MeV at Los Alamos, and for monoenergetic 14-MeV neutrons at the ICT facility. The results agree well with previous measurements at the Linac, which had covered the energy range from 1 meV to 20 MeV.

Measurements of $\bar{\nu}$ for $^{242}Am^{m}$ and ^{245}Cm were completed for neutrons of energy 14.1 MeV. The result for $^{242}Am^{m}$ agrees with a previous measurement which had been performed for energies betwen 37 keV and 30 MeV by a different method. The measurements of $\bar{\nu}$ for ^{245}Cm show a departure in the systematic trend in the dependence on bombarding energy observed for the lighter actinides. At 14 MeV $\bar{\nu}$ is about 20% lower than would have been expected from extrapolations from lighter nuclides. This change in the energy dependence of $\bar{\nu}$ may be due to a change in the path of the nuclear deformation toward scission.

Neutron Cross Section Measurements

Cross sections for the production of charged particles in reactions induced by 14-MeV neutrons are of importance to the design of fusion reactors. The energy deposited in materials as well as the radiation-induced damage depend on these cross sections. Previous measurements have investigated structural materials (e.g., Al, Ti, Fe, Ni, Cr, Cu, V, Nb, Mo, Zr) in order to estimate neutron-induced radiation damage, ^{7}Li because of its role in tritium breeding, ^{12}C because of its potential use as a protective curtain for the first wall, ^{16}O and ^{28}Si because of their use in electrical insulators. During the past year these measurements were extended to beryllium, which is often considered as a neutron multiplier to enhance the tritium breeding in the blanket of a fusion reactor, and to nitrogen, which has possible applications in refractory nitrides, as a liquid coolant, or as a part of a neutron-enhanced chemical process.

To investigate reactions induced by neutrons with energy other than 14 MeV, a magnetic quadrupole system for transporting charged particles has been installed at the cyclograaff. When this system is fully operational, it will make possible measurements on these reactions with neutrons of energies up to 34 MeV.

Although there are extensive data on proton scattering on s-d shell nuclei (mass 20 to 40), there is much less information about neutron scattering on these nuclei. An experiment on the scattering of 10- and 15-MeV neutrons on ^{24}Mg, ^{28}Si, and ^{32}S has been performed using the Bruyeres-le-Chatel neutron time-of-flight facility in order to investigate whether for target nuclei with equal numbers of neutrons and protons the same optical-model parameters describe the scattering of neutrons and protons, apart from the addition of a Coulomb potential for protons. Preliminary analysis of the elastic-scattering angular distributions at 15 MeV shows some evidence for small deviations of both the real and imaginary well depths from the values appropriate for protons. A coupled-channel analysis of the inelastic scattering to the first-excited states shows that the deformation parameters in all three cases are consistent with those obtained from proton scattering at much higher energies (~ 30 MeV).

Neutron Cross Sections Deduced from Proton Experiments

Neutron data for research applications dealing with reactors, material damage studies, shielding calculations, etc. are often obtained from optical model (OM) calculations, because measurements of neutron cross sections for many elements are not available. The parameters used in the OM potentials are obtained mainly from "global" sets (smooth dependence on mass number, energy, and neutron excess). These OM parameters predict the trend of the neutron cross sections reasonably well, but when the calculations are compared with measurements, for a given A and a given neutron energy, the values of the parameters need to be optimized to improve the agreement.

According to the Lane-model of the nucleon-nucleus OM potential, measurements of proton scattering and charge exchange (p,n) reactions to isobaric analog states (IAS) at the appropriate energy may be used to deduce neutron OM parameters.

The model has been applied to fit measurements of (p,p) elastic and (p,n) quasielastic scattering on $^{116,118,120,122,124}Sn$ at a proton bombarding energy of 24.5 MeV. The resulting OM potential parameters were then used to calculate (n,n) elastic scattering at 11 MeV for the five tin isotopes. Comparison with the Ohio University (n,n) measurements shows excellent agreement and validates the Lane-model approach for predicting (n,n) elastic scattering on the even tin isotopes.

Differential cross sections for the (p,n) reactions to the isobaric analog states (IAS) of ^{181}Ta, ^{197}Au, ^{209}Bi, ^{232}Th and ^{238}U have been measured at 26 and 27 MeV. For ^{232}Th and ^{238}U, (p,p) data at 26 MeV are also available. Coupled-channel calculations have been carried out in both proton and neutron channels and OM potential parameters for 6-8 MeV neutrons were inferred from a Lane model-consistent analysis of the data. Generally good agreement has been obtained between the calculations and the (p,p) and (p,n) data. The neutron differential elastic-scattering cross sections obtained from these calculations using the OM parameters from the proton elastic channel, as prescribed by the Lane model, have been compared with measurements available in the literature in the energy region of 6-8 MeV and with calculations obtained using neutron parameters from global sets reported at these energies. The comparisons for ^{181}Ta, ^{197}Au, and ^{209}Bi show that these neutron scattering cross sections can be predicted as well by the Lane-model approach as by neutron global parameter sets. Similar agreement was found for the neutron elastic scattering from ^{232}Th and ^{238}U at 6.5 MeV. These results support the assumption that the isospin symmetry of the Lane-model potential works as well for heavy nuclei as it does for lighter nuclei.

The same technique may be applied to (p,n) reactions to excited analog states in order to deduce information about neutron inelastic scattering. Excitation of analogs of low-lying collective states is a multistep process proceeding through inelastic excitation and charge-exchange steps. The Lane model is again used to describe the charge-exchange step; the inelastic transition is represented by the macroscopic collective model for vibrations or rotations, depending on the nucleus. The desired cross section is then obtained by a coupled-channel calculation in which several nuclear states are coupled together.

This procedure was applied to the even Se isotopes. Data for the (p,n) reaction to analogs of the ground-state and the one- and two-phonon vibrational states demonstrate that the two-phonon state must be included in the coupling for a correct calculation of the cross section for the (p,n) reaction to the one-phonon state. When this coupling is included in calculating the neutron inelastic scattering, the results agree with measurements for the lowest 2^+ state. The calculations use OM potentials which vary reasonably with mass number and which also reproduce the (p,n) data. If the two-phonon state coupling is not included, fitting the 2^+ data requires an absorption in the OM which varies by a large amount across the isotopic sequence, a much greater variation than supported by any global model. The present results show that (p,n) charge exchange reactions are indeed useful for deducing inelastic neutron scattering, provided the coupling of higher excited states is included.

Radiative Capture

For measurements on nuclear explosions using radiochemical methods a knowledge of the neutron capture cross sections of unstable nuclides is needed. Several experiments are being performed to improve the understanding of the capture process, and methods for calculating radiative capture cross sections are being developed. Measurements of capture cross sections and gamma ray strength functions are particularly useful, as are any measurements that clarify the reaction mechanism as a function of atomic weight and neutron energy. Measurements on the radiative capture of protons are easier to perform than neutron capture experiments, and the result of proton capture studies also yield useful information about neutron capture.

The reaction mechanism for the production of high-energy gamma rays ($\geq$10 MeV) in neutron or proton radiative capture reactions is expected to change from compound-nuclear to direct with increasing incident energy. The energy at which this transition takes place depends on the target nucleus, and is around 6-8 MeV for protons incident on ^{89}Y. Although this reaction has been studied extensively with NaI spectrometers, the energy resolution of these detectors has been insufficient to resolve transitions to the final states in ^{90}Zr. Hence the predictions of the reaction models could not be tested, since the test requires that the nature of the final states and the intensities of the transitions can be determined. An experiment with greatly improved resolution ($\sim$60 keV) has been performed, in which the gamma rays were detected in four germanium spectrometers. Measurements were made at a proton energy of 5 MeV, where the reaction is expected to be compound-nuclear, and at 10.5 MeV, where it should be predominantly direct. The states in

^{90}Zr that are excited at the two energies are those which would be expected on the basis of the reaction models, i.e., at 5 MeV nearly all the states up to 4 MeV are excited, whereas at 10.5 MeV only those states are observed whose configurations strongly resemble that of a proton added to the ^{89}Y target. Detailed model calculations will be required for the interpretation of the transition strengths.

The nucleon radiative capture mechanism in light nuclei was studied by performing experiments and calculations for the A = 13 system in order to increase the understanding of the differences between neutron and proton capture and to search for resonant quadrupole strength. The angular distributions of gamma rays for the $^{12}C(p,\gamma_0)$ reaction were measured with the large NaI spectrometer at proton energies between 17 and 27 MeV. A companion experiment to measure polarized neutron capture on ^{12}C is also underway at Triangle Universities Nuclear Laboratory. The excitation function for capture into the A = 13 system may be divided into two regions, the "pygmy" region between threshold and ~18 MeV and the giant dipole resonance region between 18 and 30 MeV. Calculations using the direct-semidirect (DSD) theory for E1 and E2 radiative nucleon capture. assuming only direct E2 radiation, reproduce the average behavior of the Legendre coefficients for proton capture. However, a striking deviation from the experimental Legendre coefficient a_2 occurs at 18.5 MeV. For neutron capture the average behavior of the angular distributions also agrees with experiment. However, inclusion of only direct E2 does not yield the observed fore-aft asymmetry because of the presence of resonant quadrupole strength. The DSD calculation fails to predict the magnitude for the giant dipole region but it is not clear whether the problem is with the theory or with the experiments.

Gamma-rays from the $^{159}Tb(n,\gamma)$ reaction were measured for 80 neutron resonances between 1 eV and 500 eV. Gamma-ray peaks were observed and then fitted to the spectrum associated with each resonance. The resulting array of gamma-ray intensities for each resonance provides the data from which the variation of gamma-ray strength with energy, the statistical distribution of gamma-ray widths, and correlations between gamma-ray widths and neutron widths can be obtained.

Integral Experiments

The neutron and γ-ray transport and resulting effects in large systems are usually calculated from microscopic cross sections. Because of the variety and large number of cross sections that are often required, integral experiments are of great importance to check the validity of the cross sections used in the calculations. Such experiments can also reveal errors in the computer codes.

A type of integral experiment that was developed for this purpose is the pulsed-sphere experiment in which a pulse of 14-MeV neutrons is produced at the center of a sphere of the material to be studied. The emerging neutrons are detected in a stilbene scintillator. In the most recent experiments spheres of Ho, Ta, Au, and Pb with radii between one and three mean free paths were used. The results of the measurements were compared with calculations performed with a neutron-photon Monte Carlo transport code. The cross sections used in the calculations were obtained either from the Livermore cross section file (ENDL) or the Brookhaven file (ENDF), which has independent evaluations for Au and Pb. The measured and calculated neutron spectra agree above 10 MeV for both files, but there are discrepancies below 10 MeV. Calculations based on ENDL yield 30% too many neutrons between 0.75 and 5 MeV for Ho and Ta, presumably because the assumed (n,2n) cross sections are too large, while the same calculations give 25% too few neutrons between 5 and 10 MeV for Ho, probably because too few pre-equilibrium processes were assumed. Calculations based on ENDF give 75% too few neutrons between 5 and 10 MeV for Au, again probably because of an underestimate of preequilibrium processes, and the ENDF-based calculations give 25% too few neutrons between 0.75 and 5 MeV for Pb.

In some of the pulsed-sphere experiments low-energy neutrons have been measured with a ^{6}Li glass detector. The efficiency of this detector was measured some time ago, but questions regarding the accuracy of the efficiency measurement have been raised because of apparent inconsistencies in measurements on spheres of light elements (see UCID 17271-80). An effort is underway to obtain more reliable data on the efficiency by using monoenergetic neutrons for the measurement, but the inconsistencies have not yet been resolved.

Heavy-Ion Reactions

A reaction model has been formulated for highly excited nuclei in states with high angular momenta. These nuclei are highly deformed, and the effect of this deformation on the angular momenta which emitted particles can remove and on the level densities of residual nuclei has been included in the calculations. The mass dependence of the deformation effects was studied. The calculations show an increase of cluster emission rates and a related decrease in fission probabilities when the effect of deformation was included in the calculation of the statistical decay.

A calculation of precompound emission of neutrons and protons in heavy-ion induced reactions has been performed. The calculation uses the Boltzmann master equation to predict the energy distribution of the emitted neutrons and protons as a function of time. The results of the calculation agree well with measurements for the reaction $^{16}O + ^{197}Au$.

Electron Scattering

Electron scattering probes fundamental properties of nuclei, such as the charge and magnetization distributions of nuclear ground states and the transition charge densities between the ground and excited states. Collaborative experiments with MIT have been performed at the Bates accelerator on the rare isotopes of oxygen and silicon.

The experiments showed an anomaly in the magnetization-density distribution of ^{17}O and large core-polarization effects in ^{17}O and ^{18}O. The electron scattering data were compared with the results on the scattering of 150-MeV protons by the oxygen isotopes. This comparison fixes the strength of the density-dependent terms in the effective interaction. Preliminary data have been obtained on the magnetic electron scattering on ^{29}Si. A target of ^{29}SiC has recently been fabricated which will replace the SiO_2 target that deteriorated rapidly in the earlier experiment.

Energy Levels of ^{206}Hg

Because of the importance of information on the energy levels of nuclides near A = 208 to nuclear structure models, the energy levels of ^{206}Hg were investigated. ^{206}Hg was produced in the $^{204}Hg(t,p)$ reaction with the Los Alamos tandem accelerator. Two energy levels of ^{206}Hg are known at excitation energies of 1.068 and 2.102 MeV with tentative J^{π} assignments of 2^{+} and 4^{+}. Application of the perturbed angular correlation method yielded a gyromagnetic ratio of 1.09 $\pm$ 0.01 and a life time of 3.1 $\pm$ 0.3 μs for the 2.102 MeV state. These data and theoretical considerations lead to an assignment $J^{\pi} = 5^{-}$ for this state, instead of 4^{+}.

ELECTRON AND ATOMIC PHYSICS

Atomic Collisions

The atomic physics group is studying the dynamics of ion beams moving through solids. For example, when ion beams move through solids, a large steady fraction of vacancies in atomic inner shells is produced. A detailed understanding of the mechanism which determines the steady fraction is important for the development of x-ray lasers. Auger electron yields measure the number of these vacancies. The data indicate that cross sections for collisional loss of inner shell vacancies are anomalously large. Recently the production of vacancies in the L-shell was studied. Preliminary analysis indicates that multiple vacancy processes are important.

In addition the feasibility of producing stimulated emission in a Z-pinch plasma is being explored. A possible method involves electron collisional pumping of neon-like krypton. X-ray spectra obtained on the Z-pinch Atomic Physics Project (ZAPP) and similar devices (such as Python at Physics International) indicate that large gains are expected for this system. Experiments on this system at Physics International are in progress.

Plasma Spectroscopy

The goal of the plasma spectroscopy effort is to produce a well characterized plasma which permits the study of atomic collision phenomena that are ordinarily inaccessible in the laboratory. The information is important in weapon physics, for the study of laser-produced and magnetically-confined plasmas, and for the development of x-ray lasers. Work is in progress on two plasma sources, the Tandem Mirror Experiment (TMX) and ZAPP.

The work on TMX involves two grating spectrometers, one at grazing and one at normal incidence. The spectrometers survey the line emission from the TMX plasma and serve to identify the principal impurities in the plasma. Last year these spectrometers were upgraded to provide spatial resolution (one-dimensional). The data confirmed previous interpretations of gross rotations of the TMX plasma and permitted measurements of ion temperature and of the radial electric field in the TMX plasma. While TMX is being upgraded for operation in 1982, the spectrometer detector systems are being redesigned to provide time resolution.

The effort that involves ZAPP began operation last year. The machine is capable of producing plasmas with electron temperatures above 1 keV and densities above 10^{21} cm^{-3}. Plasmas for elements ranging from carbon (Z=6) to xenon (Z=54) have been produced.

Emphasis in ZAPP is on diagnostics which currently includes a laser interferometer, an x-ray crystal spectrometer, several grating spectrometers, and x-ray pinhole photography. All these methods give spatial resolution, but integrate over time. A development program using Micro-Channel-Plates (MCP) is expected to provide nanosecond time resolution.

Channeling Radiation

Relativistic charged particles channeled in crystals, either along an axis or between planes, traverse periodic trajectories. This motion results in forward-directed emission of electromagnetic waves which, for MeV electrons, has spectral peaks in the x-ray or γ-ray portion of the spectrum. The resulting spectra have been calculated for electrons and positrons with a Monte Carlo code. The calculated spectra were compared with experiments for silicon and diamond. For silicon five discrete peaks between 30 and 125 keV were observed when 54-MeV electrons were incident on the <110> plane. For natural diamond channeling radiation was observed from a thin crystal.

The temperature dependence of the channeling radiation of electrons in a thin silicon crystal was studied to 200°C. The spectrum showed large changes with temperature. Effects of radiation damage caused by prolonged electron bombardment were also studied.

Effects of Fusion Neutrons on Thermocouples

Thermocouples are the most widely used thermal sensor in measurement and control systems. They are used in radiation damage studies of materials and in fusion confinement experiments and will undoubtedly find increased use as these experiments become more complex. Little is known about the response of thermocouples to ionizing radiation, nothing is known about the effects of 14-MeV neutrons.

An experiment was performed at RTNS-II to survey the common thermocouple alloys for fusion-neutron-induced changes in thermoelectric output. Wires of Alumel, Pt/10% Rh, Fe, Constantan, Cu, Chromel, and Pt were exposed to a fluence of $\sim 10^{18}$ n/cm^2 at room temperature. Radiation-induced effects were observed in all materials even at this low fluence. Alumel shows the largest effect in post-irradiation measurements at temperatures up to 250° C. If this radiation-induced decalibration varies linearly with fluence, Alumel would not be useful at first wall flux densities. These changes in Alumel disappear at higher temperatures (~400° C). Other materials exhibit effects which are stable to 400° C.

Positron Annihilation Analysis

A powerful method for studying the structure of solids is positron annihilation analysis. Measurements of the life time of positrons and of the doppler-broadening of the annihilation radiation can be used to determine the structure of solids as well as radiation-induced changes. Annihilation analysis has been applied to several problems.

One of the greatest difficulties in the design of a fusion reactor is the short lifetime of the wall of the plasma-containing vessel caused by radiation damage induced by 14-MeV neutrons. The selection of a suitable material requires a better understanding of the factors that influence the behavior of materials under bombardment by 14-MeV neutrons. Because of the low intensity of available 14-MeV neutron sources, irradiation with energetic protons or other charged particles can serve to simulate neutron-induced damage. Information about the most basic features of the damage process may be obtained by comparisons of the results of irradiation with both kinds of sources and measurement of the damage with positron annihilation analysis. Molybdenum samples were irradiated with protons or neutrons and then studied by positron annihilation analysis. These experiments served to study the migration characteristics of primary defects during and after irradiation. Preliminary results indicate that there are two separate migration processes: one, associated with energetic recoils, produces vacancy loops and a second, associated with low energy recoils, produces voids.

Positron analysis has also been used to study partially oxidized uranium powders. A common defect that was observed in samples prepared under diverse conditions may be part of the mechanism of oxygen transport during the oxidation process.

Another application of positron analysis has been in the study of the structure of metallic glassy alloys. Differences in structure in such alloys of different composition and changes produced by radiation were observed.

A rapidly growing research area makes use of monoenergetic, low-energy (eV) positron beams to study surface physics and positron bound state problems. At present, when positrons are produced in the decay of radioactive materials, many experiments are limited by low intensity. In experiments at the Linac, a beam of low-energy positrons was produced and detected. This technique may provide pulsed beams of low-energy positrons, orders of magnitude more intense than those presently available.

Experimental Facilities

A facility is being developed for Rutherford back-scattering (RBS) and proton-induced x-ray emission (PIXE) to study a variety of problems of interest to the Laboratory. Materials are analyzed by using the ion beam of the 3-MV electrostatic accelerator as a probe. The first analysis involved rare-earth oxide coatings on stainless steel substrates. A room-temperature surface barrier detector was used for the RBS measurements and a Si(Li) detector yielded x-ray data (down to 500 eV) for the PIXE studies. The quantitative, non-destructive technique provided thickness values and stoichiometry ratios for oxide coatings. Effects of non-uniform coatings on the RBS and PIXE results were examined.

Oxygen diffusion in olivine (Mg_2SiO_4 - type materials) was studied with an ^{18}O tracer. The ^{18}O is detected by bombardment with 3 MeV protons that induce the $^{18}O(p,n)^{18}F$ reaction. The target is beveled before bombardment so that the activity of ^{18}F across the surface gives the oxygen concentration as a function of depth.

DEVELOPMENT PROJECTS

High Power Microwaves

High-intensity electromagnetic fields in the microwave frequency range are useful for heating plasmas, for generating intense charged-particle beams, and other applications. A method is under development for filling a resonant cavity with rf energy for a relatively long time and then extracting the energy during a much shorter time to achieve a power gain.

In the first experiments difficulties arose in switching when an evacuated cavity and an electron-beam switch were used. In more recent experiments the switching was accomplished with a plasma that was formed by triggering a gas breakdown in the switch. The evacuated cavity was replaced by a cavity filled with 7 atmos. of N_2 and SF_6. With this arrangement 1.6 J of microwave energy was stored in the copper cavity during a 1.5 ms charging period and extracted in 10 ns to give output pulses of 160 MW. The stored energy was limited by the gas pressure, drive pulse length, and coupling of the feed waveguide to the cavity. These limitations can easily be relaxed to achieve higher power levels.

The plan is to employ superconducting cavities later. An attractive possibility that is under consideration is to use hemispherical rather than spherical cavities, since hemispheres are easy to fabricate and suppress some modes that would appear in spherical cavities. Experiments on spherical and hemispherical copper cavities are in progress to compare the advantages and disadvantages of the two types of cavities.

Neutron Diagnostics for Fusion Experiments

Measurement of important plasma parameters in fusion experiments is made difficult by high densities and large volumes which prevent the escape of atoms and ions from the central regions, but neutrons suffer negligible attenuation in the plasma. Knowledge of the neutron generation rate in the plasma may serve to determine primary plasma parameters, such as ion temperature, ion energy confinement time, ion density, spatial and temporal distributions of density and temperature, and may provide data for deducing the plasma power balance.

A neutron spectrometer has been developed for the Mirror Fusion Test Facility (MFTF). The spectrometer measures doppler-broadening of the neutron energy caused by the ion motion, hence permits a determination of the ion energy in the plasma. The neutron detector has a collimator to provide a spatial resolution of 10 cm at the plasma so that the spatial variation of ion energy can be mapped. A 50 ms time resolution permits determinations of confinement times. A very fast pulse height analyzer was developed to provide the needed time resolution.

Determination of Atmospheric Oxygen

Instrumentation has been developed for determining the variation of the O_2 concentration in the atmosphere with a precision of 3×10^{-6}. The purpose of the experiment is to determine the ratio of the change in O_2 concentration to CO_2 concentration to elucidate the location of the CO_2 from fossil fuel burning. Only about half the CO_2 is accounted for by the

Scripps Institute measurements of the last twenty years on the CO_2 variations in the atmosphere. The present experiment uses precision measurements of the Raman scattering intensity from N_2 and O_2 in air samples.

An overall stability of the electronics and the laser of 2×10^{-6} has been achieved with the use of a computer and a fast sampling method. Adequate intensity for the required statistical accuracy in the detection of the scattered radiation is achieved by placing the sample into the laser cavity. To eliminate sources of instability an optical system was built that permits simultaneous measurements of the O_2/N_2 ratio in an unknown and in a standard. The system is now close to meeting the requirements for measurements on samples gathered from the atmosphere.

Determination of Nitrogen in Tissue

In cooperation with the Naval Medical Research Institute nitrogen exchange in human tissues was measured. These measurements are of importance for the understanding of decompression sickness. Decompression tables are based on assumed, not measured, rates of inert gas exchange in body tissues. Previous measurements of N_2 kinetics used exhaled gas or blood.

The present experiments use radioactive nitrogen produced at the Linac as tracer. Positrons from the ^{13}N decay were detected with imaging equipment to obtain three-dimensional information on N_2 exchange. Seven persons breathed radioactive N_2 in a synthetic air mixture for 30 minutes. The ^{13}N emissions were recorded during the inhalation and the subsequent 90 minutes. Measurements over regions of head, neck, shoulder, and knee show different nitrogen exchange rates in different tissues. Data from the knee joint indicate that the ^{13}N activity continued to increase even after breathing of the radioactive gas had been discontinued for some time.

PUBLICATION LIST - JOURNAL ARTICLES

(July 1980 - June 1981)

"Study of Electrofission and Hadron-Induced Fission Decay of the Giant Quadrupole Resonance of ^{238}U," J.D.T. Arruda-Neto and B.L. Berman, Nucl. Phys. A349, 483 (1980)

"Test of E2 Virtual-Photon Spectra Calculated in the Distorted-Wave Born Approximation," J.D.T. Arruda-Neto, B.L. Berman, S.B. Herdade, and I.C. Nascimento, Phys. Rev. C 22, 1794 (1980)

"E2 Giant Resonances and an M1 Component in the Photofission of ^{236}U," J.D.T. Arruda-Neto, S.B. Herdade, B.L. Berman, and I.C. Nascimento, Phys. Rev. C 22, 1996 (1980)

"Fission Decay of the Giant Quadrupole Resonance for ^{234}U," J.D.T. Arruda-Neto, B. L. Berman, S. B. Herdade, and I. C. Nascimento, Phys. Rev. C 23, 2595 (1981).

"Measurement of the Neutron-Induced Fission Cross Sections of Americium-241 and Americium-243 Relative to Uranium-235 from 0.2 to 30 MeV," J.W. Behrens and J.C. Browne, Nucl Sci. Eng. 77, 444 (1981)

"Photoneutron Cross Section for ^{4}He," B.L. Berman, D.D. Faul, P. Meyer, and D.L. Olson, Phys. Rev. C 22, 2273 (1980)

"Observation of Radiation from $\Delta n = 3$ Transitions for Planar-Channeled Electrons,", B.L. Berman, S.D. Bloom, S. Datz, M.J. Alguard, R.L. Swent, and R.H. Pantell, Phys. Lett. 82A, 459 (1981)

"Precompound Decay in Heavy-Ion Reactions," M. Blann, Phys. Rev. C 23, 205 (1981)

"A Monte Carlo Method for Calculating Strength Functions in Many-Fermion Systems," S.D. Bloom, S.M. Grimes, and R.F. Hausman, Phys. Lett. 93B, 227 (1980)

"Neutron-Capture Cross Sections for Osmium Isotopes and the Age of the Universe," J.C. Browne and B.L. Berman, Phys. Rev. C 23, 1434 (1981)

"Radiative Decay of the 2p $^{2}P_{3/2,1/2}$ States of Lithiumlike Krypton (Z=36) and the 2s2p $^{3}P_{1}$ State of Berylliumlike Krypton," D.D. Dietrich, J. A. Leavitt, H. Gould and R. Marrus, Phys. Rev. A 22, 1109 (1980)

"Fe, Kr and Nb X-ray Spectra Produced in 8.5 MeV amu^{-1} Ion-Solid Collisions," R.J. Fortner, R.H. Howell and D.L. Mathews, J. Phys. B: Atom. Molec. Phys. 13, 3545 (1980)

"Quasimolecular Inner-Shell Charge-Transfer Cross Sections for Light Projectiles in Solids," J.D. Garcia, R.J. Fortner, H.C. Werner, D. Schneider, N. Stolterfoht, and D. Ridders, Phys. Rev. A 22, 1884 (1980)

"Anomalous Optical Potential for Sub-Coulomb Barrier Protons," S.M. Grimes, Phys. Rev. C 22, 436 (1980)

"Shell Model Test of the Porter-Thomas Distribution," S.M. Grimes and S.D. Bloom, Phys. Rev. C 23, 1259 (1981)

"Charged-Particle Emission in Reactions of 15-MeV Neutrons with ^{89}Y, ^{90}Zr, and ^{92,94,95,96}Mo," R.C. Haight, S.M. Grimes R.G. Johnson, and H.H. Barschall, Phys. Rev. C 23, 700 (1981)

"Measurements and Calculations of the Neutron Emission Spectra from Materials Used in Fusion-Fission Reactors," L.F. Hansen, C. Wong, T.T. Komoto, B.A. Pohl, and R.J. Howerton, Nucl. Technology 51, 70 (1980)

"*Fission Neutron Multiplicity for the ^{242m}Am(n,f) Reaction*," R.E. Howe, J.C. Browne, R.J. Dougan, R.J. Dupzyk, and J.H. Landrum, Nucl. Sci. Eng. 77, 454 (1981)

"Positron-Lifetime Study of Copper Irradiated by d-T Fusion Neutrons," R.H. Howell, Phys. Rev. B 22, 1722 (1980)

"Signatures of Density Dependence in the Two-Nucleon Effective Interaction near 150 MeV," J. Kelly, W. Bertozzi, T.N. Buti, F.W. Hersman, C. Hyde, M.V. Hynes, B. Norum, F.N. Rad, A.D. Bacher, G.T. Emery, C.C. Foster, W.P. Jones, D.W. Miller, B.L. Berman, W.G. Love, and F. Petrovich, Phys. Rev. Lett. 45, 2012 (1980)

"States in ^{14}C from σ_T and $\sigma_{el}(\theta)$ for ^{13}C + n: Measurement, R-Matrix Analysis, and Model Calculations," R.O. Lane, H.D. Knox, P. Hoffman-Pinther, R.M. White and G.F. Auchampaugh, Phys. Rev. C 23, 1883 (1981)

"Evidence for a Strongly Deformed Prolate Shape at N=87 from ^{154}Eu and ^{152}Eu(p,t) Reactions," R.G. Lanier, G.L. Struble, L.G. Mann, W. Stoffl, I.C. Oelrich, J. Scheerer, I.D. Proctor, D.W. Heikkinen, and R.H. Howell, Phys. Lett. 99B, 23 (1981)

"Two-Level Model for Inner-Shell Excitation: Effect of Translation Factors," S.J. Pfeifer and J.D. Garcia, Phys. Rev. A 23, 2267 (1981)

Neutron Total Cross Section for Tritium," T.W. Phillips, B.L. Berman, and J.D. Seagrave, Phys. Rev. C 22, 384 (1980)

"A Measurement of the ^{18}O Photonuclear Cross Sections as a Test of a Bremsstrahlung Unfolding Technique," R.E. Pywell, M.N. Thompson, and B.L. Berman, Nucl. Instrum. Methods 178, 149 (1980)

"K-and L-Shell Vacancy Sharing Between Light Projectiles and Argon Targets," K.J. Reed, J.D. Garcia, R.J. Fortner, N. Stolterfoht, and D. Schneider, Phys. Rev. A 22, 903 (1980)

PUBLICATION LIST - CONFERENCE REPORTS

(July 1980 - June 1981)

"Generation of High-Power Microwave Pulses Using a Spherical Superconducting Cavity and Interference-Type Switch," R.A. Alvarez, D. Birx, D. Byrne, M. Mendonca, and R.M. Johnson, International Conference on Applied Superconductivity, Santa Fe, NM, September 1980; IEEE Trans. Magn. MAG-17, 935 (1981)

"Decay of the E2 Giant Resonance for $^{234,236,238}U$ by Fission," J.D.T. Arruda-Neto, B.L. Berman, S.B. Herdade, and I.C. Nascimento, Giant Multiple Resonance Topical Conference, Oak Ridge, TN, October 1979; Harwood Academic Publishers, New York, p. 433 (1980)

"A Test of E2 Virtual-Photon Spectra," J.D.T. Arruda-Neto, B.L. Berman, S.B. Herdade, and I.C. Nascimento, International Conference on Nuclear Physics, Berkeley, CA, August 1980; Lawrence Berkeley Laboratory Report LBL-11118, p. 268 (1980)

"Production of Photon Beams Useful for Nuclear Physics from Channeling Radiation," B.L. Berman, Symposium on Perspectives in Electro- and Photonuclear Physics, Saclay, France, September 1980; Saclay Report DPh-N/HE/81/2, p. 5 (1981)

"Electromagnetic Dissociation of Relativistic Heavy Ions: A Photon Target," B.L. Berman, Symposium on Perspectives in Electro- and Photonuclear Physics, Saclay, France, September 1980; Saclay Report DPh-N/HE/81/2, p.7 (1981)

"ZAPP: An Inexpensive Versatile X-Ray Source," D.D. Dietrich, R.J. Fortner, D.F. Price and R.E. Stewart, 1980 Conference on the Application of Accelerators in Research and Industry, Denton, TX, November 1980; IEEE Trans. Nucl. Sci. NS-28, 1366 (1981)

"Photodisintegration of Three-Body Nuclei," D.D. Faul, B.L. Berman, P. Meyer, and D.L. Olson, International Conference on Nuclear Physics, Berkeley, CA, August 1980; Lawrence Berkeley Laboratory Report LBL-11118, p. 68 (1980)

"A New Parameterization of the E1 Gamma-Ray Strength Function," D.G. Gardner and F.S. Dietrich, International Conference on Nuclear Cross Sections for Technology, Knoxville, TN, October 1979; Nat. Bur. Stand. Spec. Publ. 594, p.770 (1980)

"A Study of Source Neutron Reactions," P. Grabmayr, J. Rapaport, R.W. Finlay, V. Kulkarni, and S.M. Grimes, International Conference on Nuclear Cross Sections for Technology, Knoxville, TN, October 1979; Nat. Bur. Stand. Spec. Publ. 594, p. 542 (1980)

"Neutron Cross Sections for Fusion," R.C. Haight, International Conference on Nuclear Cross Sections for Technology, Knoxville, TN, October 1979; Nat. Bur. Stand. Spec. Publ. 594, p. 228 (1980)

"Status of (n, charged particle) Measurements at LLL," R.C. Haight and S.M. Grimes, Symposium on Neutron Cross Sections from 10 to 50 MeV, Brookhaven National Laboratory, May 1980; Brookhaven Report BNL-NCS-51245, Vol. I, p. 245 (1980)

"Neutron Scattering Cross Sections for ^{232}Th and ^{238}U Inferred from Proton Scattering and Charge Exchange Measurements," L.F. Hansen, S.M. Grimes, B.A. Pohl, C.H. Poppe, and C. Wong, Symposium on Neutron Cross Sections from 10 to 50 MeV, Brookhaven National Laboratory, May 1980; Brookhaven Report BNL-NCS-51245, Vol.II, p. 781 (1980)

"The Transport of 14-MeV Neutrons Through Heavy Materials", L. F. Hansen, T. T. Komoto, B. A. Pohl, and C. Wong, 1981 Annual Meeting of the American Nuclear Society, Miami Beach, FA, June 1981; Trans. ANS 38, 567 (1981).

"RTNS-II: Present Status," D.W. Heikkinen and C.M. Logan, 1980 Conference on the Application of Accelerators in Research and Industry, Denton, TX, November 1980; IEEE Trans. Nucl. Sci. NS-28, 1490 (1981)

"Tritium Experience at RTNS-II," C.M. Logan, J.C. Davis, T.A. Gibson, D.W. Heikkinen, B.J. Schumacher, and M.S. Singh, ANS National Topical Meeting on Tritium Technology in Fission, Fusion and Isotopic Applications, Dayton, OH, April 1980; U.S. Department of Energy Document CONF-800427, p. 372 (1980)

"Coulomb Dissociation of ^{18}O," D.L. Olson, B.L. Berman, D.E. Greiner, H.H. Heckman, P.J. Lindstrom, G.D. Westfall, and H.J. Crawford, International Conference on Nuclear Physics, Berkeley, CA, August 1980; Lawrence Berkeley Laboratory Report LBL-11118, p. 220 (1980)

"Characteristics and Applications of Channeling Radiation from Relativistic Electrons and Positrons," R.H. Pantell, R.L. Swent, S. Datz, M.J. Alguard, B.L. Berman, and S.D. Bloom, 1980 Conference on the Application of Accelerators in Research and Industry, Denton, TX, November 1980; IEEE Trans. Nucl. Sci. NS-28, 1152 (1981)

"The Experimental Observation of Isovector Giant Quadrupole Strength in ^{16}O," T.W. Phillips and R.G. Johnson, Giant Multipole Resonance Topical Conference, Oak Ridge, TN, October 1979; Harwood Academic Publishers, New York, p. 461 (1980)

"A Study of Optical Model Parameters for High Energy Neutron Cross Sections from 5 to 50 MeV in the Mass-140 Region," T.W. Phillips, H.S. Camarda, and R.M. White, Symposium on Neutron Cross Sections from 10 to 50 MeV, Brookhaven National Laboratory, May 1980; Brookhaven Report BNL-NCS-51245, Vol. II, p. 769 (1980)

"Photonuclear Cross Sections of ^{29}Si and ^{30}Si," M.N. Thompson, R.E. Pywell, P. Kean, G. Odgers, and B.L. Berman, International Conference on Nuclear Physics, Berkeley, CA, August 1980; Lawrence Berkeley Laboratory Report LBL-11118, p. 862 (1980)

"Direct Nitrogen Exchange Measurements in Multiple Human Tissues," P.K. Weathersby, P. Meyer, E.T. Flynn, and L.D. Homer, Undersea Medical Society Annual Scientific Meeting, Asilomar, CA, May 1981; Undersea Biomedical Research 8, No.1, Supplement, p. 35 (1981)

"Fission Cross Section of ^{245}Cm from 10^{-3} eV to 10^{4} eV," R.M. White, J.C. Browne, R.E. Howe, J.H. Landrum, and J.A. Becker, International Conference on Nuclear Cross Sections for Technology, Knoxville, TN, October 1979; Nat. Bur. Stand. Spec. Publ. 594, p. 496 (1980)

E-DIVISION SCIENTIFIC STAFF

Permanent Staff

R. A. Alvarez

R. W. Bauer, Division Leader

J. A. Becker

B. L. Berman (on research leave August 1980 - August 1981)

H. M. Blann

S. D. Bloom (also Department of Applied Science, University of California, Davis)

R. Booth

D. D. Dietrich

F. S. Dietrich

R. J. Fortner

S. M. Grimes (left March 1981)

R. C. Haight, Assoc. Div. Leader

L. F. Hansen

D. W. Heikkinen

R. E. Howe

R. H. Howell

T. T. Komoto

R. E. Marrs (started October 1980)

G. J. Mathews (started April 1981)

P. Meyer

T. W. Phillips

B. A. Pohl

C. H. Poppe, Assoc. Div. Leader

I. D. Proctor

D. P. Rowley (started May 1981)

D. R. Slaughter

R. M. White

M. A. Williamson

C. Wong

J. G. Woodworth

Visiting Faculty Members (Summer)

H. H. Barschall, Wisconsin

H. S. Camarda, Pennsylvania State

B. J. Dalton, Iowa State

T. W. Donnelly, M.I.T.

R. W. Finlay, Ohio

J. D. Garcia, Arizona

J. W. Jury, Trent (Canada)

A. K. Kerman, M.I.T.

H. W. Lefevre, Oregon

V. A. Madsen, Oregon State

K. G. McNeill, Toronto (Canada)

F. L. Petrovich, Florida State

R. E. Pywell, Melbourne (Australia)

M. N. Thompson, Melbourne (Australia)

Channeling radiation

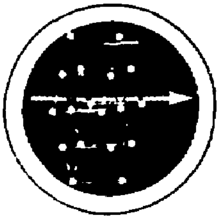

For further information contact
Barry L. Berman or
Stewart D. Bloom (422-4519)

In collaboration with scientists at Stanford University and Oak Ridge National Laboratory, we have confirmed the existence of channeling radiation, that is, x rays emitted when high-energy electrons or positrons pass through a crystal along one of its planes or axes. We first observed these x rays several years ago (although we did not identify their source at the time) during experiments designed to test whether we could improve our photonuclear experiments with positron annihilation radiation by suppressing the bremsstrahlung background by using a low-Z crystal as the annihilation target. Channeling radiation is intense, monochromatic, polarized, and emitted primarily in the forward direction. These unique characteristics suggest that it might become a valuable tool for probing the structure of crystals and other solid-state systems as well as for the study of photonuclear reactions. It might also some day prove useful as a medical diagnostic tool.

Many of the experimental uses of visible light depend upon the ease with which it can be polarized, directed, or split into monochromatic bundles. However, scientists have been forced to accept x rays more or less as they come (i.e., in a jumble of wavelengths too penetrating to be affected by ordinary polarizers, lenses, mirrors, or monochromators). Hence the discovery of channeling radiation—intense x rays that are polarized, highly directed, and monochromatic—opens up numerous experimental possibilities.

Although we did not recognize it at the time, we first observed channeling radiation in 1968 while we were looking for something else. We were studying photonuclear reactions with x rays produced by the annihilation of ultrarelativistic positrons from our linear accelerator, and we hoped to improve these measurements by suppressing the ever-present background of bremsstrahlung x rays. Since positron annihilation takes place in the electron cloud between the atoms, whereas bremsstrahlung originates largely in the Coulomb field close to the atomic nuclei, we reasoned that we could suppress bremsstrahlung by using a thin crystal of some light element such as lithium or beryllium as the annihilation target. If we aligned the crystal carefully with the incoming positron beam, the positrons would be likely to find clear channels in the crystal structure through which they could penetrate deeply and in which they would spend most of their time far from the atomic nuclei.

The experimental results justified our expectations.[1,2] The positrons did follow channels in the crystal, and the bremsstrahlung was suppressed (Fig. 1). At the same time, however, we noticed an unexpected intense background of x rays in the sub-100-keV energy range. This radiation did not hinder our experiments (a sheet of lead stopped it), but we still had no satisfactory explanation of its origin.

We thought at the time that this anomalous radiation had to be coherent bremsstrahlung, although there was more of it than would be expected under the existing theory. Ordinary bremsstrahlung arises when a positron or an electron transfers momentum to an individual nucleus in a single collision. Coherent bremsstrahlung arises at those angles of incidence that allow the charged particle to transfer momentum to an array of periodically bound nuclei (a whole crystal), again in a single collision.

Extensive theoretical and experimental investigations of coherent bremsstrahlung have been carried out with high-energy electrons (above about 1 GeV) at several accelerator centers, but ours is the only laboratory that has investigated this phenomenon at more modest energies (below about 100 MeV). We were able to identify coherent bremsstrahlung coming from our crystal targets, but there was still an additional low-energy background radiation that defied interpretation.

Finally, in 1975-76, scientists at Stanford University and in the U.S.S.R. predicted the emission of channeling radiation from crystals bombarded with positrons. In response to these predictions, we embarked upon the present series of experiments in 1978 in collaboration with scientists from Stanford University and Oak Ridge National Laboratory. Within a short time we were able to show that the persistent low-energy x-ray background we had been observing was channeling radiation.

Particle channeling

Particle channeling was first discovered about 20 years ago in connection with heavy particles. When a well-collimated beam of heavy ions is directed along an axis or plane of a crystal, the ions find themselves in "clear" channels surrounded by regular arrays of atoms. In this situation the ions become transversely trapped as a result of many sequential collisions. This results in anomalously high transmission and low energy losses of the ion beam passing through the crystal.

More recent research has expanded the subject to include relativistic charged particles and has provided a quantitative picture of how they behave in penetrating a crystal lattice. In these experiments, we bombarded thin slices of silicon crystal with electrons or positrons and measured how the numbers of particles that came through varied as we tilted the crystal. Figure 2 shows a schematic

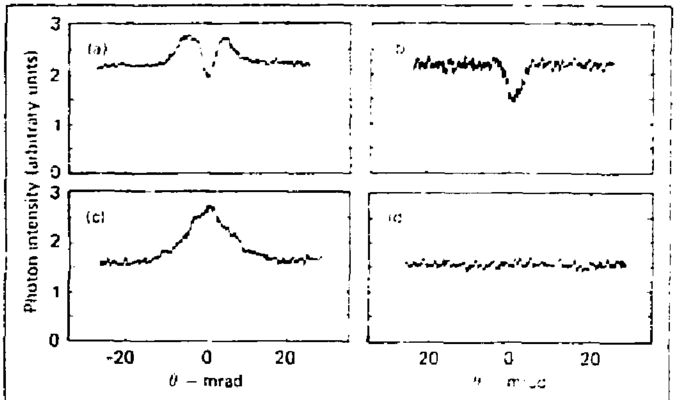

Fig. 1. *Our first observation of channeling radiation was made in the course of ionization chamber measurements of x rays generated by 28-MeV charged particles channeled along the 110 axis of a 53-μm silicon crystal. With positrons bombarding the crystal, we obtained the data shown in (a). The central dip is the expected suppression of bremsstrahlung. The enhanced radiation on both sides (i.e., the wings) was thought at the time to be coherent bremsstrahlung, but it was later shown to be channeling radiation. In a repeat positron bombardment (b) we covered the ionization chamber with a 1-cm sheet of lead, thus eliminating the low-energy radiation of the wings. Later, when we bombarded the crystal with electrons (c), no central dip was observed, but the low-energy background was still present in the central hump. In a repeat electron bombardment, with a 1-cm sheet of lead covering the ionization chamber as in (b), we obtained the results shown in (d), demonstrating that the hump in (c) was due to low-energy radiation (< 100 keV) in the wings of (a).*

Fig. — Results of charged-particle-transmission experiments. (a) Experimental arrangement used to measure the effect of tilting the silicon crystal. The detector is sensitive to both electrons and positrons. (b) Strong blocking and sharp peaking of anomalous positron transmission observed upon scanning through the 110 axis of an 18-μm-thick silicon crystal. The high collimation of the positron beam (to 1.5 mrad) was a critical factor in producing this effect. (c) Multiple valleys and peaks in the transmitted positron beam caused, respectively, by blocking and anomalous transmission in connection with various crystal planes in the same crystal. The scan was through the (110) plane about 50 mrad off the 110 axis, and the beam was not as well collimated (4 mrad) as in (c). (d) Electron transmission through a 9-μm silicon crystal, with the scan passing through the 111 axis. The electrons were highly collimated (0.5 mrad). The anomalous transmission is almost hidden by the strong blocking.

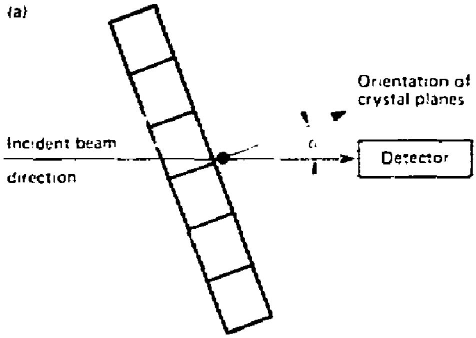

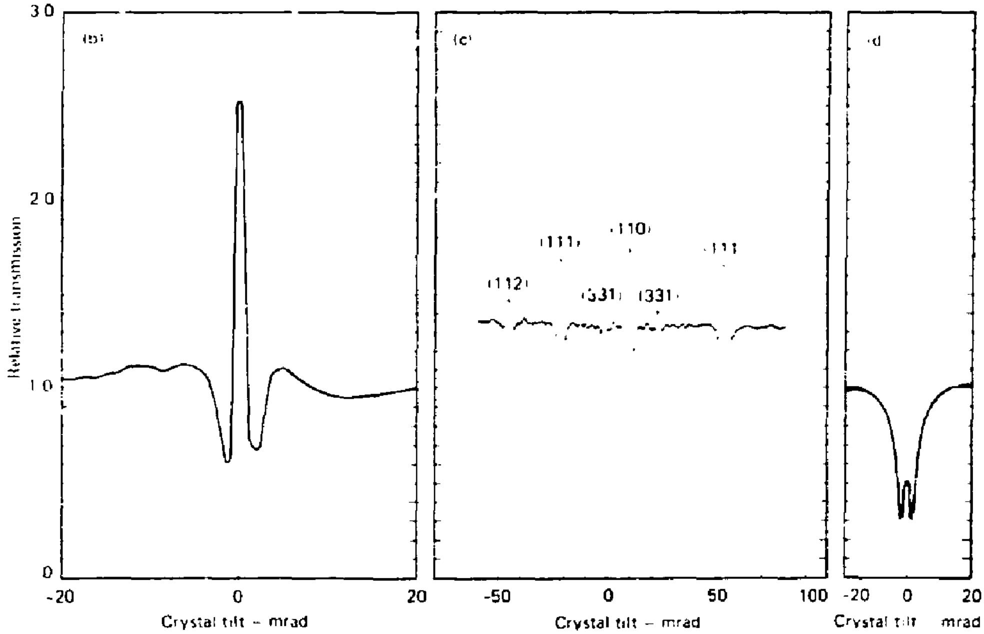

diagram of the experimental setup and several examples of such measurements, made under a variety of conditions. The tilts in these experiments are small, in no case more than 100 mrad (about 6°) on either side of some principal crystal plane or axis.

Figure 2b shows the result of a transmission experiment with a well collimated (about 1.5 mrad) beam of 56-MeV positrons in which we scanned through the ⟨110⟩ axis of an 18-μm thick silicon crystal. If we start with the crystal axis aligned with the positron beam, the particles find clear channels, and many more of them can get through to the detector (anomalous transmission) than would be the case with poorly collimated positrons and an arbitrarily oriented crystal. If we turn the crystal 20 mrad in either direction, the positrons encounter an essentially random array of nuclei through which a few would manage to thread their way (normal transmission). In between, with the crystal axis only slightly misaligned with the beam, the positrons encounter dense arrays of atomic nuclei, which block them by greatly increasing their chance of missing the detector as a result of a large angle collision.

Figure 2c shows the results of a similar experiment with positrons in which the scan passes though the (110) plane of an 18-μm-thick silicon crystal but at 50 mrad away from the ⟨110⟩ axis. Since the widths of planar channels are smaller than the widths of axial channels, the peaks and dips of the transmission scans are shallower than in Fig. 2b. The multiple extra peaks come from anomalous transmission through additional preferred directions in the crystal.

Figure 2d shows the result of a charged-particle-transmission experiment in which we used 56-MeV electrons instead of positrons, collimated to less than 0.5 mrad, incident upon a 9-μm silicon crystal. The scan is through the ⟨111⟩ axis in a direction roughly perpendicular to the (110) plane.

It is not intuitively obvious why there should be channeling in this case, since the electron is negatively charged, and the nuclei attract it. However, there is a narrow region in the vicinity of each "wall" of the channel between the atomic planes where the electron is strongly attracted by the nuclei but glances off of them in small angle collisions, much like a flat rock skipping across the water. This leads to oscillatory channeling just as for positrons, but in this case the blocking region and the channeling region coincide. Thus for an electron the blocking effect far outweighs the anomalous transmission. Comparing this figure with 2b clearly illustrates the difference in anomalous transmission between electrons and positrons. This difference is borne out by an order of magnitude difference in their measured effective coherence lengths, i.e., the observed degree of monochromaticity of the channeling radiation each of these channeled particles emits.

Channeling radiation

To understand the origin of channeling radiation, imagine yourself following the positron at nearly the velocity of light as it threads its way between two planes of a crystal. To the right and the left, row upon row of massive atomic nuclei, all positively charged, flash by. The positron, also positively charged and hence repelled by the nuclei, tends to follow the midplane between the rows. Whenever it strays to one side or the other, the repulsion of the nuclear charge turns it back. The positron therefore becomes trapped in the channel, though oscillating slightly from side to side as it travels.

Just as an oscillating dipole radiates, so an oscillating charge generates electromagnetic radiation, in this case x rays, at right angles to its direction of oscillation. Furthermore, since every positron has the same side-to-side oscillation, the x rays are polarized. We can also explain the frequency and monochromaticity of these x rays in classical terms, but it is more realistic if we invoke quantum mechanics.

Because of the relativistic contraction and the relatively slow oscillations (compared with the forward velocity), from the positron's standpoint the crystal is very much foreshortened, and the electrostatic fields of its individual nuclei blend together into the composite electrostatic potential shown in Fig. 3a.[10,11] Quantum mechanics allows the positron to occupy any of the levels indicated by horizontal lines and to move from one to the other by absorbing or emitting radiation. Because the shape of the potential is almost exactly that of a harmonic oscillator, the levels are almost evenly spaced and each of these transitions takes almost the same amount of energy and hence corresponds to almost the same wavelength of light. The result is that the positron, oscillating in its channel, emits highly monochromatic polarized radiation directed along its line of travel (Fig. 3b). As can be theoretically predicted and as we have shown, the energy of this x radiation is proportional to the 3/2 power of the positron energy.[12]

We have observed channeling radiation at several different wavelengths when we have bombarded the crystal with electrons. This result had not been predicted before our experiment and cannot

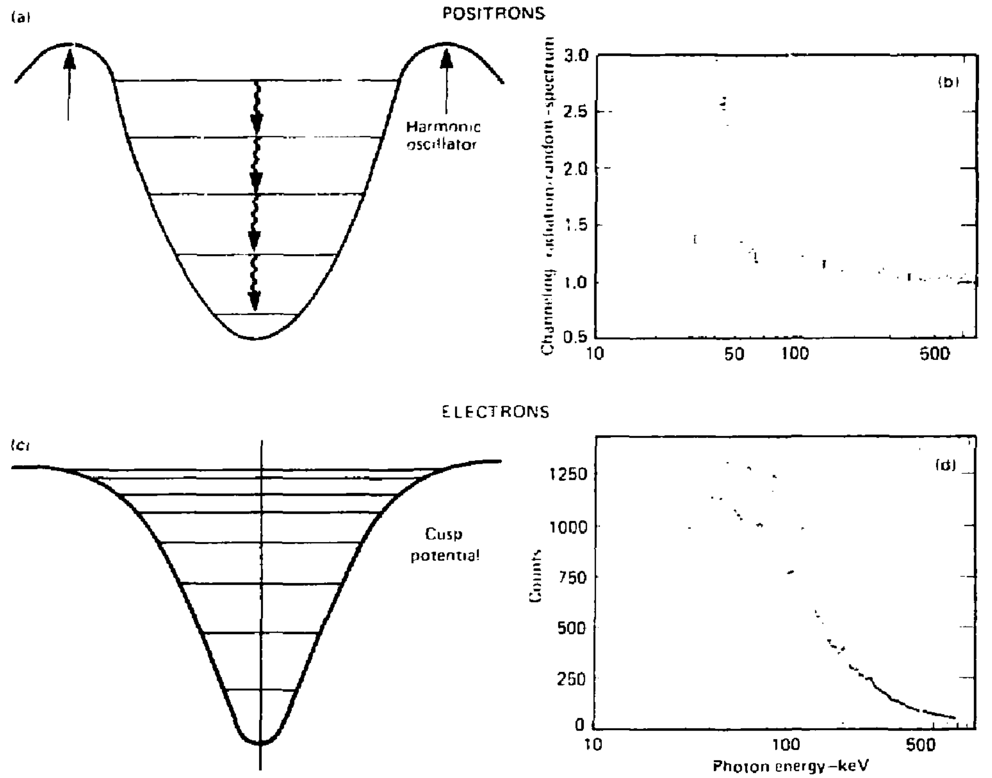

Fig. *Relativistic positrons and electrons channeled along one of the planes of a crystal produce channeling radiation. (a) Electric fields acting on a relativistic positron repel it from both sides, producing motion that is essentially that of a harmonic oscillator. The even spacing of the energy levels implies that a transition from one to another will always involve the same amount of energy and hence the same wavelength of radiation (in this case x rays). (b) Ratio of the channeling radiation to a random spectrum for 56-MeV positrons incident upon an 18-μm-thick silicon crystal, aligned with the (110) plane, showing the single large peak. (c) Electric fields acting on a relativistic electron. The electron is attracted by the nuclei and can channel through the crystal as a consequence of many small-angle scattering events. The narrow channel it traverses is characterized by a cusp-shaped potential, and the energy levels are nonuniformly spaced, leading to emission of several discrete wavelengths instead of one. (d) Radiation from 56-MeV electrons incident upon the same 18-μm-thick silicon crystal, aligned with the (110) crystal plane, showing the multiple peaks characteristic of the electron channeling radiation.*

be easily explained in classical terms. In quantum mechanical terms, however, the crystal plane or axis is no longer a wall but rather an attractive potential with the cusp shape shown in Fig. 3c. The spacing of the energy levels in such a potential is nonuniform, leading to a number of discrete wavelengths in the emitted radiation (Fig. 3d). Experiments here and elsewhere have confirmed this cusp model and furnished its parameters.[10-12]

The intensity of the channeling radiation from electrons is much lower than that from positrons. This is partly because the energy of the channeling radiation from electrons is divided among several different wavelengths and partly because the radiation from the electrons is characterized by a much shorter *effective coherence length* than that from the positrons, i.e., the electrons are knocked out of their trapped motion much sooner than the positrons. (This phenomenon is called "dechanneling.") The positrons stay near the center of the channel, where they are relatively unlikely to hit the walls, and hence give rise to radiation with an effective coherence length of 5 to 15 μm on the average.[illegible] (The effective coherence length is essentially the same as the mean dechanneling length.) The electrons are attracted to the lattice planes or axes where they are fairly certain to have an early large-angle dechanneling collision with a nucleus that has moved slightly out of line. Hence the effective coherence length of their radiation is only about 1 μm.[10,13]

Roughly speaking, in the frame of reference of an observer following the charged particle through the crystal, the channeling x rays would be emitted equally forward and backward. In the frame of reference that includes the crystal, the detector, and the laboratory, however, the charged particle is moving at almost the speed of light. This high relative velocity compresses almost all the radiant energy into a narrow forward cone. The half angle of this cone is about $1/\gamma$, where γ is the ratio of the particle's kinetic energy to its rest mass. For 56-MeV charged particles, γ is 110, and the half-angle of the forward radiation cone is about 9 mrad.

Ideally the x rays from channeling positrons would be strictly monochromatic (all have the same energy). In practice the energy varies slightly with angular divergence from the beam axis, because of the angle-dependent Doppler effect as well as the departure from the pure harmonic oscillator potential (see Fig. 3a). Hence the measured energy spread depends upon the divergence of the positron beam and the angular aperture of the detector. For electrons the detector aperture effect is negligible in comparison with the effects of the short effective coherence length.

Experiment

Figures 4a and 4b are schematic diagrams showing the essentially similar experimental setups for particle-transmission and channeling-radiation measurements. Standard bending and focusing magnets bring the charged-particle beams, produced in our electron–positron linear accelerator,[14] to the experimental area. We usually use 56-MeV (and sometimes 28-MeV) beams with average intensities in the 100-pA range, pulsed at 1440 Hz.

The quadrupole magnet focuses the collimated and magnetically analyzed charged particles to a divergence sometimes less than 0.5 mrad at the target crystal. (The magnetic analysis reveals an energy spread in the range 0.1% to 1.0%.) A three-axis goniometer with remotely controlled stepping motors holds the crystal and tilts it in 60 μrad steps.

For particle-transmission experiments we demagnetize the dump magnet and measure the forward-transmitted intensity with a small movable plastic scintillation detector. Then we tilt the crystal progressively along various angular directions and observe the effect on the scintillator signal. The resulting transmission measurements provide a map of the major crystal axes and planes.

To measure the channeling radiation, we energize the dump magnet to deflect the electrons or positrons (Fig. 4b) and replace the cesium iodide scintillator with a high-resolution intrinsic or lithium-drifted germanium photon detector. To monitor the deflected positron or electron beam without putting too many background x rays into the experiment, we direct the beam to a large paddle-shaped plastic scintillator detector located at the bottom of a 5-m-deep hole in the floor. We also insert a collimator between the dump magnet and the photon detector to restrict the detector's view to the central part of the crystal, and sometimes we add another collimator just before the photon detector to reduce the background further and improve the angular resolution.

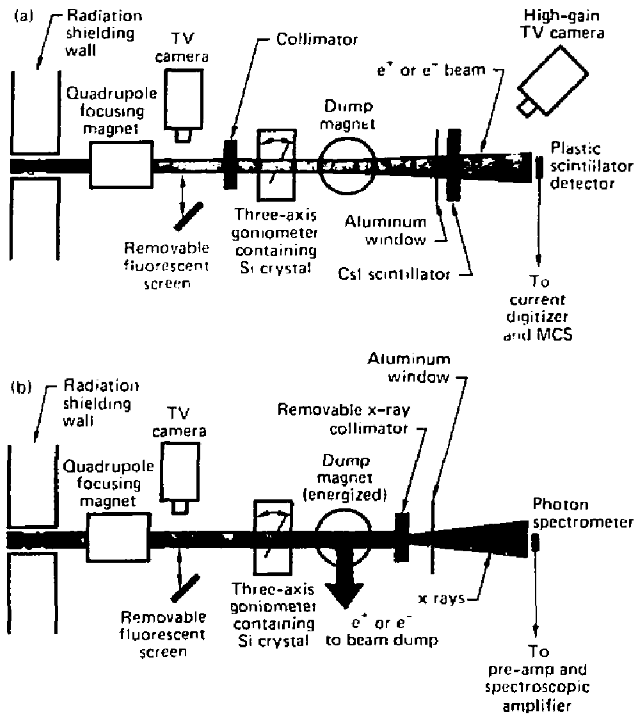

Fig. 4 *Experimental arrangements for measuring (a) charged-particle transmission and (b) channeling radiation. In charged-particle-transmission experiments, the charged-particle beam from the linear accelerator passes first through a quadrupole magnet that focuses it and a collimator that removes stray particles. The first television camera then views the removable fluorescent screen for preliminary beam focusing. Next, the beam passes through the silicon crystal (held in the remotely controlled three-axis goniometer), the dump magnet (turned off and demagnetized), and the aluminum exit window. It then enters the cesium iodide scintillator (viewed by the high-gain television camera) for final alignment and collimation. During transmission measurements, we withdraw the cesium iodide scintillator and monitor changes in the transmitted beam, as a function of crystal tilt, with a plastic scintillation detector. To measure channeling radiation (b), we turn on the dump magnet and direct the electron or positron beam into a 5-m-deep hole in the floor. With the charged particles out of the way, it is then possible to detect the channeling x rays with a lithium-drifted germanium photon detector.*

The most critical parameter in these experiments is the divergence of the incident charged-particle beam. The low duty factor (i.e., the ratio of beam on-time to beam off-time) of the linear accelerator makes it necessary to use very weak beams of electrons and positrons (50 to 500 pA) to avoid pileup of the detected events. This makes it almost impossible to locate and view the beam (necessary for fine-tuning the focus) by ordinary methods. Hence we have developed a novel technique.

We insert a thallium-activated cesium iodide scintillator into the beam after the aluminum window and view it with an ultrasensitive television camera. A color quantizer encodes the television image, assigning different colors to areas of different brightness. Figure 5 displays the dramatic difference between the off-channel and on-channel cases, illustrating the efficacy of this experimental technique and the great sensitivity to small changes in crystal orientation or in beam-tuning parameters.

This sensitivity allows us to achieve the best experimental conditions possible with the available beam-line configuration and beam-transport components at the linear accelerator facility. Over the past year, and particularly after the realignment made necessary by our recent earthquake, we have improved the attainable beam focusing from a divergence of several milliradians in late 1978 to less than 0.5 mrad in our two latest runs. For further experimental details see Ref. 15.

Applications

Because we have only recently discovered channeling radiation and determined some of its properties, any discussion of its potential applications is of course tentative. Nonetheless, several research areas under investigation appear promising enough to merit a brief review.

In theory, channeling radiation from positron bombardment is intense, monochromatic, highly directed, and polarized. We have experimentally demonstrated the first three of these properties, and we hope to conduct experiments soon to demonstrate the polarization property. Any fruitful application should hinge on one or more of these properties.

Because of all of its properties, particularly intensity and monochromaticity, channeling radiation is of interest as a probe in the study of atomic, molecular, and crystalline structure where sources of radiation in the keV range with these properties are scarce or nonexistent. For example, phase transitions in crystals could be studied by monitoring the characteristics of the channeling radiation at varying macroscopic quantities like pressure and temperature. Channeling radiation in the keV range would even be of interest in photonuclear studies involving excitation of the low-lying collective

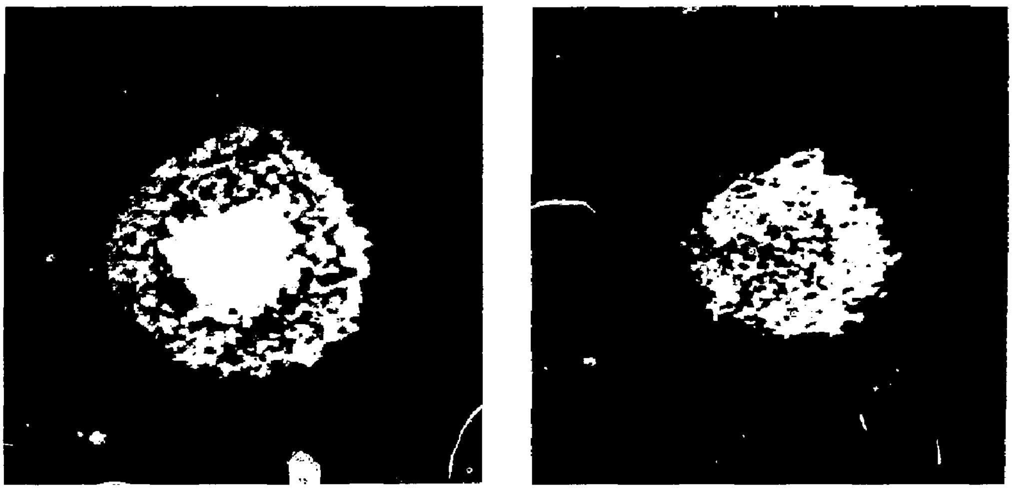

(a) (b)

Color representation of the brightness pattern of a beam of 56-MeV positrons after it has passed through an 18-μm-thick silicon crystal (recorded with the cesium iodide scintillator and high-gain television camera). (a) The diffuse pattern formed when the crystal was oriented in a random direction with respect to the positron beam. (b) The sharper and more intense pattern formed when the ⟨110⟩ axis of the crystal was accurately aligned with the beam. This experimental technique was useful in achieving the precise alignment of the crystal and the high directional uniformity (low divergence) of the charged-particle beam necessary for observations of channeling radiation.